JOURNAL OF MATERIALS SCIENCE 25 (1990) 2095–2099

Medium range order in high surface area amorphous silicas

R. MANAILA*, M. ZAHARESCU‡
*Institute of Physics and Technology of Materials, Bucharest, Magurele, P.O.B. MG 7, Romania
‡Research Centre for Physical Chemistry, Bucharest, Romania

Medium-range order (MRO) in amorphous (a-) SiO_2 can be defined as the degree of orientational correlation between neighbouring $SiO_{4/2}$ tetrahedra. Analysis of X-ray diffraction data on high surface area a-silicas shows that the MRO can be characterized quantitatively by means of (a) the first peak position in the interference function and (b) the ratio between O–O(II) and Si–O(II) coordination heights in the pair distribution function. These two quantities are physically related.

1. Introduction

Medium-range order in amorphous silicas prepared by different methods is still a matter of controversy. Short-range order (SRO) is chemically determined as the $SiO_{4/2}$ tetrahedron. On the other hand, medium-range order (MRO) relates to the spatial linking of these tetrahedra and can be defined as the degree of orientational correlation between them. MRO is fully characterized by the distribution of Si–O–Si and dihedral angles [1, 2]. While SRO is acknowledged to be practically the same in different varieties of a-SiO_2, including the vitreous one, MRO seems to be much more sensitive to the preparation method and hydration degree. Also, MRO can be expected to influence the chemical and rheological properties of the silicas.

Recently, evidence was put forward for the presence of "internal surfaces" in a-SiO_2, more specifically of zones with a high defect concentration [3, 4], which could explain certain features in the Raman absorption spectra and in the thermal properties. At these defect-rich internal boundaries, chemical bonds are likely to "reconstruct" in order in minimize the free energy, thereby altering the bulk MRO [3–5].

On the other hand, in silica gels, vacuum-deposited films and porous a-SiO_2 Himmel *et al.* [6–8] found by X-ray diffraction an α (low T)-cristobalite-type MRO. Thermal annealing around 250° C was shown [6] to induce a displacive α–β transition, affecting the MRO. This transition is accompanied, in the case of gels, by densification and elimination of OH residues.

This work intends to look further into possible MRO models for high surface area amorphous silicas with different hydration degrees, obtained by different methods.

2. Experimental procedure

A series of commercial powdered amorphous silicas were investigated by X-ray diffraction. The samples fell into several classes, by the method of preparation, microstructure and hydration degree: pyrogenic, precipitated, xero- and aerogels.

The distribution of scattered intensity was recorded with Mo$K\alpha$ radiation until $k = 4\pi \sin\theta/\lambda \simeq 150\,\mathrm{nm}^{-1}$. Monochromatization was achieved by a bent quartz crystal, placed in the diffracted beam, before the scintillation counter. Data were processed by a computer program, which applied corrections for scattering by air, polarization by sample and monochromator, transmitted incoherent and multiple (double) scattering, as well as for the thermal background of the scintillation counter. The incoherent intensity $I_{inc}(k)$, scattered by the SiO_2 sample, was calculated in an analytical approximation [9]. The transmission function $Q(k)$ of the monochromator was evaluated after Ruland [10]. The energy window of the monochromator and a k-independent background were used as adjustable parameters, in order to obtain minimal spurious ripples in the pair distribution function $G(R)$, in the range $R < 0.1$ nm. This procedure allows for the actual deviations of the necessary corrections from those calculated (mostly by analytical approximations). Restricted zones of the pattern were also recorded with Cu$K\alpha$ radiation.

3. Interference function

Fig. 1a shows an interference function $i(k)$, typical for high surface area a-SiO_2 powders. It is defined as

$$i(k) = (\alpha I_{cor}(k) - I_{ind}(k))/f_{el}^2(k)/\langle Z\rangle^2$$

where α is a scaling factor, I_{cor} the corrected intensity, $I_{ind}(k) = \langle f(k)^2\rangle + Q(k)I_{inc}(k)$, $f(k)$ the atomic scattering factor, $f_{el}(k)$ the average electronic scattering and Z = the electron number. The average is taken over the compositional unit.

The interference function comprises five main peaks up to $k_{max} = 132.0\,\mathrm{nm}^{-1}$, where the Fourier integration was limited, due to the high statistical noise at higher k. As can be seen in Fig. 1a, $132\,\mathrm{nm}^{-1}$

0022–2461/90 $03.00 + .12

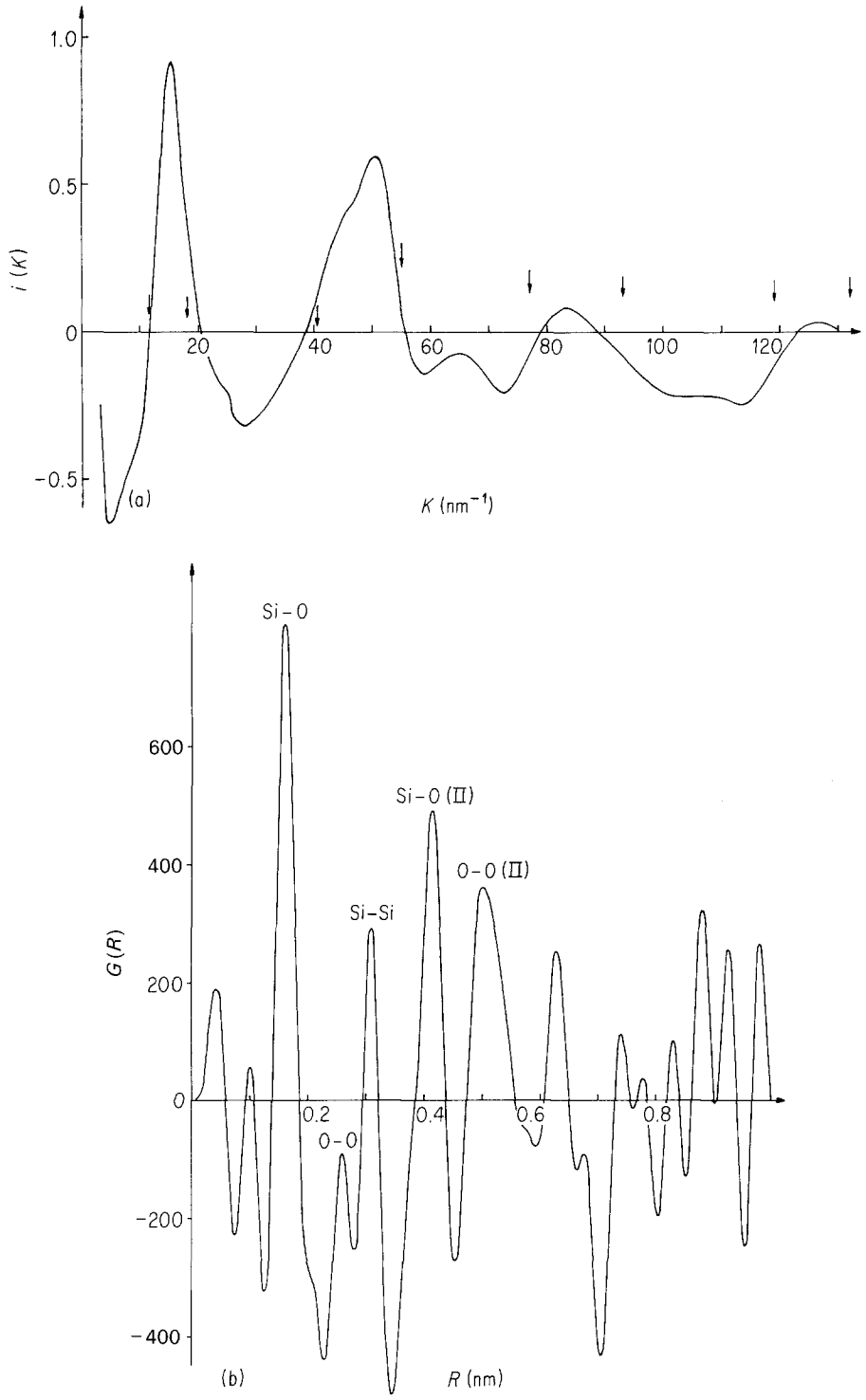

Figure 1 (a) Interference function of an Aerosil 200 sample. ↓: k values for which $i(k) = 0$ (after [6]). (b) Pair distribution function for the same sample.

corresponds to $i(k) \simeq 0$, in agreement with recent determinations of the a-SiO_2 structure [2, 6], thus reducing the end-of-series spurious ripples in the real space transform. The general $i(k)$ aspect is very similar in v-SiO_2 and amorphous pulverulent silicas, so that we must look into details of the interference function, which could reflect distinct features of the MRO.

4. Position of the first intensity peak

The position of the first peak (k_1) in the interference function was found to differ among the samples investigated. In the following, the k_1 values referred to were derived from raw $I_{obs}(k)$ data, rather than from $i(k)$ ones. The systematic difference between k_1 values derived from $I_{obs}(k)$ and $i(k)$ is small in comparison with the experimental accuracy and does not alter the relative situation of the samples. The experimental k_1 values range between 15.4 to 16.6 nm^{-1} for different pulverulent silicas (Fig. 2), as compared with $k_1 = 15.2 \pm 0.10\,nm^{-1}$ in v-SiO_2. It is interesting to note in Figs 2 and 3 that the commercial Syloid gels span the k_1 range reported in [6] for silica gels, from as-precipitated samples ($k_1 \simeq 16.5\,nm^{-1}$) to gels annealed up to 800° C ($k_1 \simeq 15.2\,nm^{-1}$). Most of our amorphous silicas are concentrated in the k_1 range 15.4 to 15.9 nm^{-1}.

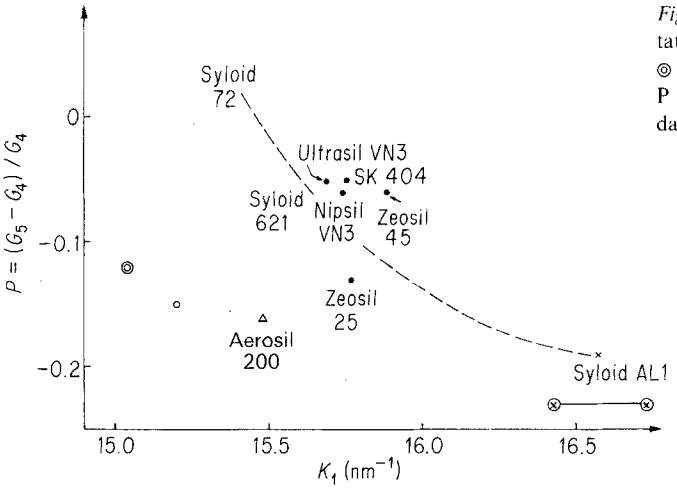

Figure 2 k_1 and $P = (G_5 - G_4)/G_4$ values for a-silicas: ● precipitated, × Syloid 72 and Syloid 621 gels, △ pyrogenic, ○ vitreous, ◎ v-SiO_2 [6–8], ⊗ range for silica gels (as-obtained from TEOS) [6]. P values are calculated from the heights of the $G(R)$ peaks (our data) and of the $C(R)$ peaks (data from [6]).

These abnormally high k_1 values (as referred to v-SiO_2) should be related to a medium-range order which differs from that in v-SiO_2. This difference might rest on the following.

(1) A different type of tetrahedra linking into more-or-less well defined clusters, similar to those occurring in the crystalline SiO_2 forms, as proposed by Himmel *et al.* [6–8].

(2) The linking of the tetrahedra is similar to that in v-SiO_2, but includes zones where the orientational correlation between neighbouring tetrahedra is disturbed (internal defect-rich zones or external surface of primary particles).

5. Pair correlation function

The physical significance of the k_1 shift can be traced back to the $G(R)$ pair distribution function

$$G(R) = 4\pi R^2 \sum_i \sum_j c_i K_i K_j (\varrho_{ij}(R) - c_j \varrho_0)$$

where c_i and K_i are concentration and effective electron number of species i, $\varrho_{ij}(R)$ is the numerical density of j atoms at a distance R from an i atom and ϱ_0 is the average atom density.

Fig. 1b shows a $G(R)$ function typical for a-SiO_2 samples, in which coordinations are identified, belonging to the SRO range ($R < 0.30$ nm) and to the MRO range ($R \geqslant 0.30$ nm).

It can be shown that the first $i(k)$ peak is particularly sensitive to interatomic distances at 0.4 to 0.5 nm. They give their strongest (sin kR)/kR maximum at $kR = 7.73$, i.e. at $k = 19.3$ to 15.5 nm^{-1}, which is precisely the range spanned by the k_1 values. This range of interatomic distances comprises the Si–O(II) coordination (around 0.4 nm, which also contains some O–O(II) pairs) and the O–O(II) one (around 0.5 nm, also containing some Si–Si(II) pairs). If the 0.5 nm $G(R)$ peak (G_5) decreases in height, in comparison with the 0.4 nm one (G_4), the first $i(k)$ peak will be shifted towards larger k_1 values. A convenient characterization of the relative height of G_5 and G_4 is the ratio $P = (G_5 - G_4)/G_4$ [11].

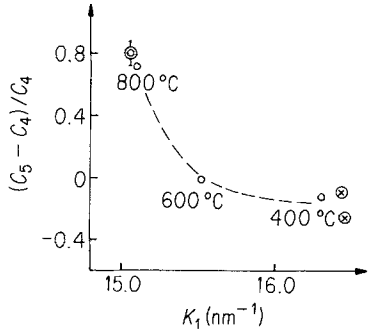

Figure 3 k_1 and $P = (C_5 - C_4)/C_4$ values ($C(R)$ = correlation function) for silica gels [6] as-obtained from TEOS (⊗) and annealed (○). ◎: v-SiO_2. Data taken from figures in [6].

The correlation between P and k_1 can be followed on Fig. 2, where the high-k_1 samples are generally seen to display lower G_5 coordination heights (lower P ratios). A decrease in height originates in a broadening of the coordination peak, indicative of a disturbed correlation at this distance.

A simple model calculation (Section 6 below) shows that the O–O(II) coordination is much more broadened than the Si–O(II) one, when the coupling between neighbouring tetrahedra is "broken" (when orientational correlation of the tetrahedra is weakened).

It is worth mentioning here that in neutron-irradiated SiO_2 glass Doi [12] has reported a similar reduction in height of the 0.5 nm peak, in comparison with the 0.43 nm one, as a result of strong induced structural disorder.

It results that the k_1 positive shift in a-silicas could be assigned to a decrease in height (broadening) of the G_5 coordination, i.e. to increased inter-tetrahedra disorder (reduced MRO).

It can be seen on Fig. 2 that the xerogels Syloid 72 and 621 show increased MRO, in comparison with the desiccant gel Syloid AL 1, considering both the k_1 and P values. The precipitated silicas Ultrasil VN3, Nipsil VN3, Zeosil 25, Zeosil 45 and SK 404 are similar, both concerning their k_1 and their $(G_5 - G_4)/G_4$ values and lie close to a curve $P(k_1)$ describing the gels. The pyrogenic Aerosil 200 shows a lower P ratio, similar to that measured in v-SiO_2. P values calculated for TEOS-derived fresh gels on the basis of Himmel *et al.* [6] data (Fig. 2) are slightly lower than the values measured in commercial silicas for the same k_1 range, maybe due to the fact that they were based upon the correlation function, instead of the pair distribution one.

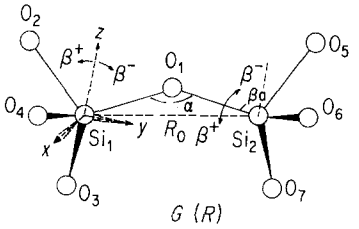

Figure 4 Possible mutual position of two neighbouring $SiO_{4/2}$ tetrahedra.

The relationship between k_1 and $(G_5 - G_4)/G_4$ is clearly illustrated by the data of Himmel *et al.* [6] on gels, as-prepared and annealed up to the vitrification point (Fig. 3). Here, the correlation function

$$C(R) = \tfrac{1}{2}\pi^2 R \int_{k_{\min}}^{k_{\max}} I_{\text{cor}}(k) \sin kR \, dk,$$

used by the authors, was employed in calculating P, instead of $G(R)$. Fig. 3 illustrates the gradual increase of MRO in silica gels upon thermal annealing. It can be viewed as a gradual homogenization of the network by the formation of additional intertetrahedra links, which enhance the O–O(II) G_5 coordination. Thus, the as-prepared gels seem to be comprised of small, relatively ordered regions separated by thick disordered boundaries, which interrupt the silica network and accommodate OH, H_2O and organic residues. Thermal annealing causes an ordering process in these boundaries, accompanied by dehydration, the volume fraction of the ordered network increasing up to that in v-SiO_2. Porous glass and evaporated a-SiO_2 films were shown [8] to be similar to the fresh TEOS gels, as concerns the k_1 values.

6. A crude model of MR disorder in a-silica

The simplified model sketched in Fig. 4 allows a calculation of the Si–O and O–O distances for any relative position of two neighbouring tetrahedra.

Assuming a complete decoupling, the tetrahedra were given the possibility to take independently, with a certain probability, any rotational position around a given direction in space, while preserving the positions of the Si_1 and Si_2 atoms. The rotation angle β (in Fig. 4 rotation is around an axis normal to the plane of the paper) was assumed to be distributed Gaussian-like around the ideal network value β_0.

The coordinates of the atoms and their mutual distances were calculated in a cartesian reference system, with the origin in the Si_1 ion. For the sake of simplicity, the plane of the Si–O–Si bonds (the plane of Fig. 4) was chosen as the $(1\,\bar{1}\,0)$ plane in our cartesian reference system and the angle Si–O–Si was assigned the value 144.05°, close to the maximum of the experimental α distribution in a-SiO_2 [1].

Combinations of several particular situations were envisaged:

(i) the rotation of the two tetrahedra occurs in the same sense (variant A) or in an opposite sense (variant B),

(ii) the tetrahedra are rotated around the $[1\,\bar{1}\,0]$ (variant I, illustrated in Fig. 4) or $[1\,1\,0]$ (variant II) direction.

The halfwidth of the β angle distribution characterizes the degree of orientational correlation between tetrahedra and is related to the degree of disorder in that region of the network. In the Gaussian distribution: $P(\beta) = 1/[\sigma(2\pi)^{1/2}] \exp -(\beta - \beta_0)^2/2\sigma^2$, σ was tentatively assigned the value 9.4, which corresponds to a half-height width of the distribution of 21.5°. The specific value assigned to σ does not influence the course of our argument.

The β_0 ideal values are dependent upon the chosen α value. As an example, for our choice (α = 144.05°) and for the rotation around the $[1\,\bar{1}\,0]$ axis, β_0 resulted as O for the Si_1 tetrahedron and +58° for the Si_2 one.

Fig. 5a exemplifies the distribution $D(R)$ of the Si_1–O_5 and Si_1–O_6 distances for tetrahedra rotated in the same sense around the $[1\,\bar{1}\,0]$ direction (variant AI). The other Si–O separations are equal, in this case, to one of these two distances. The sum of all Si–O distances appears as a broad distribution, centred upon the "ideal" values corresponding to $\beta = \beta_0$ (indicated in Fig. 5a by vertical bars). The sum distribution of O–O distances is broader, but still centred upon the main ideal distance (0.511 nm).

Rotation in the opposite sense around either $[1\,\bar{1}\,0]$ or $[1\,1\,0]$ directions (variants BI and BII) brings about a considerably larger broadening of the O–O distance distribution (Fig. 5b), in comparison with the Si–O one. The O–O distribution becomes very flat and its centre is shifted towards smaller distances, in comparison with the ideal distribution.

Thus, a randomized mutual position of "decoupled" neighbouring tetrahedra is able to induce a strong broadening of the O–O pair correlation at $\simeq$0.50 nm, while the Si–O correlation is less affected.

It should be said that some interatomic distances

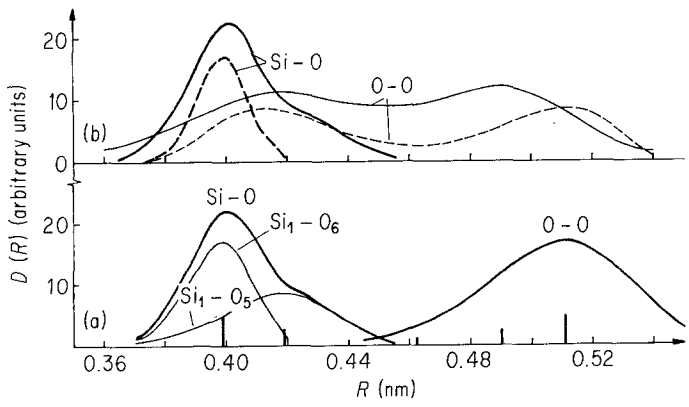

Figure 5 Distribution of the Si–O(II) and O–O(II) distances in three variants of orientational disorder (see text) of two neighbouring tetrahedra. (a) variant AI, (b) —— variant BI, – – – variant BII. Vertical bars: distances in an "ideal" configuration (no rotational disorder).

(e.g. O_3–O_5 in variant BI) prove to be little sensitive to orientational disorder. However, they cannot be expected to show up as peaks at the ideal positions because of the additional disorder affecting the distance between tetrahedra centres. The Si_1–Si_2 distance was assumed in the argument above to be constant at the $R_0 = 0.322$ nm value, which corresponds to the chosen $\alpha(144.05°)$. Nevertheless, this distance can also be the subject of Gaussian fluctuations, which would additionally broaden the calculated distance distributions. The O–O sum distribution is more sensitive in this respect than the Si–O one, as was suggested by a calculation performed with R_0 increased by 10%. In this case, the width of the total O–O distribution increased by $\simeq 5\%$, while that of the Si–O distribution did not change significantly.

Thus, an impaired correlation between neighbouring tetrahedra (MR disorder) causes indeed a stronger broadening (and decrease in height) of the O–O(II) coordination (G_5), in comparison with the Si–O(II) one (G_4). Thereby, MR disorder is related to a decrease of the P ratio and a shift of the k_1 interference peak towards larger values.

7. Conclusions

The position of the first peak (k_1) in the intensity distribution of amorphous silicas is informative about their degree of medium-range order, by reference to vitreous SiO_2. The k_1 value is determined by the ratio P between the O–O(II) and Si–O(II) coordinations, which is related to the degree of medium-range order (orientational correlation between neighbouring $SiO_{4/2}$ tetrahedra).

The P and k_1 values were used in the present work in an attempt to quantify the degree of medium-range order in high surface area amorphous silicas, prepared by different methods, in comparison with the vitreous material.

References

1. R. L. MOZZI and B. E. WARREN, *J. Appl. Crystallogr.* **2** (1969) 164. J. R. G. DA SILVA, D. G. PINATTI, C. E. ANDERSON and M. L. RUDEE, *Phil. Mag.* **31** (1975) 713.
2. P. A. V. JOHNSON, A. C. WRIGHT and R. N. SINCLAIR, *J. Non-Cryst. Solids* **58** (1983) 109.
3. J. C. PHILLIPS, *J. Non-Cryst. Solids* **34** (1979) 153.
4. *Idem, Phys. Rev.* **B24** (1981) 1744.
5. R. MANAILA and R. GRIGOROVICI, *J. Non-Cryst. Solids* **97–98** (1987) 195.
6. B. HIMMEL, TH. GERBER and H. BURGER, *ibid.* **91** (1987) 122.
7. B. HIMMEL, TH. GERBER, W. HEYER and W. BLAU, *J. Mater. Sci.* **22** (1987) 1374.
8. B. HIMMEL, TH. GERBER and H.-G. NEUMANN, *Phys. Status Solidi a* **88** (1985) K127.
9. F. HAJDU, *Acta Crystallogr.* **A28** (1972) 250.
10. W. RULAND, *Br. J. Appl. Phys.* **15** (1964) 1301.
11. R. MANAILA and M. ZAHARESCU, *Phys. Status Solidi a* **98** (1986) 377.
12. K. DOI, *J. Non-Cryst-Solids* **51** (1982) 367.

Received 4 January
and accepted 23 August 1989